Mixed Bennett Vorticity:
A hybrid family of nonlinear Shear-Flow Stabilized Z-pinch equilibria

Matt Russell

A family of Shear-Flow Stabilized vortical equilibria was found by studying the Bennett Pinch, and a cubic temperature case was investigated for the situation made by exchanging the classic Bennett nonlinearity between the density and flow profile, with calculations made that compared favorably with contemporary measurements, and profiles from the ZaP, FuZE, and Zap-HD experiments. The nonlinearity can also be distributed between the two quantities, so long as it is done so in a way that leaves the structure of the Bennett Current invariant from its cubic vortex form. The distribution which maximizes and minimizes the shear is studied.

INTRODUCTION

Bennett profiles[1][2] have historically described a class of Z-pinch equilibria who possess a nonlinear density profile,

$$n(r) = \frac{n_0}{(1+\xi^2 r^2)^2} \tag{1}$$

where following off of Bennett we can define,

$$\xi^2 = bn_0 \tag{2}$$

as a normalizing quantity with the dimension of an inverse length squared. The Bennett parameter for a two-fluid system,

$$b = \frac{\mu_0 e^2 u_0^2}{8k_B(T_e + T_i)} \tag{3}$$

is a characteristic parameter describing a fluid plasma with separate temperatures for electrons and ions, and a uniform flow velocity, as well as a core plasma (number) density of n_0.

In the ideal limit, $R_m = \mu\sigma uL \to \infty$, and from a magnetohydrodynamic perspective this means that $T = T_e \simeq T_i$, so

$$b = \frac{\mu_0 e^2 u_0^2}{16k_B T} = \frac{C_B}{T} = (1.45697 * 10^{-22})\frac{u_{z,0}^2}{T} \tag{4}$$

Despite the presence of a $\sim \frac{1}{r^4}$ nonlinearity in the plasma density it turns out that the fluid equations of an ideal plasma, i.e., Ideal Magnetohydrodynamics (MHD) can be solved exactly in the case of an axisymmetric equilibrium. Meaning, here, one that is symmetric both azimuthally and axially, because the governing partial differential equations (PDE) describing the equilibrium reduce to an integrable system of ordinary differential equations (ODE) expressing the typical fluid conservation laws augmented by the appropriate form of Maxwell's equations.

This analytic nature to the classic Bennett Pinch is critical because it means that if we swap the density and flow profiles, i.e.,

$$n(r) \to n_0 \tag{5}$$

$$u_{z,0} \to u_z(r) = \frac{u_{z,0}}{(1+\xi^2 r^2)^2} \tag{6}$$

where $u_{z,0}$ is of course the amplitude of the core plasma flow, then the current density remains unchanged while now representing a flow state which is non-uniform, i.e., vortical.

This non-zero vorticity is more than just a mathematical curiosity. In the axisymmetric case, and for a purely axial flow, it naturally expresses a flow shear,

$$\vec{w} = \nabla \times \vec{u} = w_\theta \hat{\theta} = -\frac{\mathrm{d}u_z}{\mathrm{d}r}\hat{\theta} \tag{7}$$

This is relevant as modern fusion science enjoys the advantage of the Shear-Flow Stabilized Z-Pinch[3], which is a form of the Z-Pinch that can be stabilized against the $m = 0$, and $m = 1$ instabilities naturally plaguing the device[4][5]. When the flow shear is great enough, a quasi-equilibrium appears which is stable for several orders of magnitude longer than the predicted lifetime of a static Z-pinch[6][7], and which evidently attributes its stability to the shear-flow stabilization mechanism.

MOTIVATION

Investigation into pinch-based plasma physics is an active field of inquiry, and largely has been since the early days of research into the physics and engineering of plasma reactors for producing energy from the fusion of light atoms. Modern research into this subject is a rich scientific business whose major projects command expensive computer time for simulation and analysis campaigns which must be waged in order to understand the output from the fusion plasma diagnostics attached to the large, high-voltage, high-powered, experimental systems which generate the plasma, and cause the magnetic pinch(es) to occur[8][9].

Alongside this, a theoretical understanding of pinch behavior is naturally required in order to interpret the experimental observations. Modern investigations of this kind center around, and are enriched, both by the presence of nonlinear physics, as well as the subject of plasma turbulence, due to the form that the natural evolution of the pinch plasma frequently takes in experiments. Although the vortical equilibrium plasma flow which is the subject of this research paper is not the same thing, strictly-speaking, as a form of strong or weak MHD tur-

bulence, the notion of vorticity is fundamentally entangled with the study of turbulence[10][11]. Obtaining shear-flow stabilization conditions to a nonlinear, vortical, ideal plasma equilibrium is interesting for a multitude of reasons, both in of itself and as a platform for further work on the science of SFS Z-Pinches.

It is also of particular interest that the current density profile of the Bennett Pinch is the flow state under consideration here. The Bennett Pinch is one of the oldest topics in plasma physics, with perhaps only Langmuir and ionospheric Whistler waves being older. Studying the conditions on this form for shear-flow stabilization in the ideal limit is of interest in general as this limit merely corresponds to the shear being positive definite.

BACKGROUND

Research into fluid dynamics is one of the most active fields of modern physics as it brings together a wide range of scientific discplines, and offers a rich variety of problems to researchers. When the electrical conductivity of the fluid is considered then the finite electric and magnetic fields which exist as a consequence of the flow of electric charge must be incorporated into the governing equations of fluid dynamics, and the range of possible behaviors expands.

In the ideal limit, which can be interpreted as meaning no magnetic diffusivity $\lambda = (\mu\sigma)^{-1}$, or more thoroughly, an infinite magnetic Reynold's number,

$$R_m = \sigma\mu u L \tag{8}$$

then the magnetic field acts as if it were "frozen-in" to the plasma, meaning that it is transported along with the plasma flow. The basic mechanism behind this arises from nature's abhorrence for a change in the magnetic flux of a system. Consequently, an equilibrium MHD plasma can be treated as a magnetic spring, because, in the absence of magnetic diffusion the only dynamics which are observable are the ones induced by a displacement from the magnetic equilibrium according to Lenz's law. In other words, to keep the magnetic flux the same, any arbitrary change in the field at any point in the plasma will arbitrarily induce currents in the plasma volume of such a form so as to counteract this change via their self-generated magnetic fields.

Ideal Magnetohydrodynamics

Ideal MHD, which is of course the aforementioned ideal limit to magnetohydrodynamics and hereafter referred to just as MHD for the rest of the scope of this paper, is the simplest form that a system of governing equations for the behavior of an electrically-conducting fluid can meaningfully take. A "first-principles" derivation of this system, starting from taking suitably-closed moments of kinetic equations describing the evolution of one-particle distribution functions for each plasma species in a full 6D+t phasespace, before appropriately reducing the resulting set of fluid equations to the ideal limit, is outside the scope of this article.

Instead, a satisfactory expression for the homogeneous form of the system is provided below for when there are no inhomogeneities present, e.g., collisions, external sources of mass, momentum, or energy, etc.. The ideal gas law which is commonly used to close the moment-taking process is included at the end, and note that in Equation (15) the electrons are assumed to carry the current, with immobile ions,

$$\frac{\partial\rho}{\partial t} + \nabla\cdot(\rho\vec{u}) = 0 \tag{9}$$

$$\frac{\partial\rho\vec{u}}{\partial t} + \nabla\cdot(\rho\vec{u}\vec{u} - \frac{\vec{B}\vec{B}}{\mu_0} + (p + \frac{B^2}{2\mu_0})\underline{\underline{I}}) = 0 \tag{10}$$

$$\frac{\partial\vec{B}}{\partial t} + \nabla\cdot(\vec{u}\vec{B} - \vec{B}\vec{u}) = 0 \tag{11}$$

$$\frac{\partial e}{\partial t} + \nabla\cdot((e + p + \frac{B^2}{2\mu_0})\vec{u} - \frac{\vec{B}\cdot\vec{u}}{\mu_0}\vec{B}) = 0 \tag{12}$$

$$\rho \simeq m_i n \tag{13}$$

$$e = \frac{p}{\gamma - 1} + \frac{\rho\vec{u}\cdot\vec{u}}{2} + \frac{B^2}{2\mu_0} \tag{14}$$

$$\vec{J} = -ne\vec{u} \tag{15}$$

$$\vec{E} = -\vec{u}\times\vec{B} \tag{16}$$

$$p = 2nk_BT \tag{17}$$

The above system of eight nonlinear, hyperbolic, partial differential equations expresses the evolution of mass, momentum, energy, and magnetic field in a flat spacetime, at non-relativistic speeds, and they are coupled to relations for the current density, electric field, plasma pressure, plasma mass density, and internal energy. Together Equations (9) - (17) completely describe the ideal behavior of a fluid plasma in arbitrary geometry.

Axisymmetric MHD Equilibrium

When a homogeneous MHD flow is steady, meaning it features no quantities which depend on time, then the governing equations simplify, and they now express strong conditions for there being no divergence of the flux associated with any conservative MHD variable. Additionally, if the flow is cylindrical, and axisymmetric, meaning in the context of a cylindrical flow that its properties depend only on the radial coordinate, then it possesses both an axial, and azimuthal symmetry, and the equations simplify even further because all the axial and azimuthal derivatives vanish from the equations.

Ordinarily, the bulk plasma flow is taken to be static, i.e., $\vec{u} = 0$, or uniform, $\vec{u} = u_0\hat{u}$, in order to simplify the LHS of the momentum equation so that the force balance rests entirely on the Lorentz force and plasma pressure

gradient. When the bulk plasma flow is instead nonuniform, then the equilibrium is that of a dynamic one, and there are three equations which largely define dynamic, cylindrical, axisymmetric MHD equilibria[12],

$$\nabla \cdot \vec{B} = 0 \tag{18}$$

$$\nabla \times \vec{B} = \mu_0 \vec{J} \tag{19}$$

$$\rho \vec{u} \cdot \nabla \vec{u} = \vec{J} \times \vec{B} - \nabla p \tag{20}$$

with the difference in general between the dynamic and the static case being contained in the convective term that now shows up on the LHS of Equation (20). This term vanishes if the plasma flow is uniform, of a perturbative amplitude, or in certain equilibrium cases, e.g., a flowing Z-pinch[13]. Then it becomes,

$$\frac{\mathrm{d}p}{\mathrm{d}r} = -J_z B_\theta \tag{21}$$

Z-Pinch

The Z-pinch is the simplest possible axisymmetric configuration for magnetically confining a plasma whereby the Lorentz force of an axial plasma current, and the associated azimuthal magnetic field compresses ("pinches") the plasma inward against the outward-directed plasma pressure gradient,

$$\vec{J} = J_z(r)\hat{z} \tag{22}$$

$$\vec{B} = B_\theta(r)\hat{\theta} \tag{23}$$

$$\nabla p \to \frac{\mathrm{d}p}{\mathrm{d}r}\hat{r} \tag{24}$$

according to Equation (20). Note that the LHS of this equation, i.e., the convective non-linearity term, will be identically zero for an arbitrary Z-pinch equilibrium because the radial transport of momentum due to the advection of flow gradients through the pinch goes to zero. In general, this term reads,

$$(\vec{u} \cdot \nabla \vec{u})_r = u_r \frac{\partial u_r}{\partial r} + \frac{u_\theta}{r}\frac{\partial u_r}{\partial \theta} + u_z \frac{\partial u_r}{\partial z} - \frac{u_\theta^2}{r} \tag{25}$$

from the above it is obvious why this term will be 0 for an axisymmetric Z-pinch.

When fusion research was first declassified internationally in the 50s researchers believed, largely on the back of the Z-pinch's simplicity, and buoyed by the rousing success of controlling fission, that igniting a Z-pinch would be a simple task. However, this was not the case as the Z-pinch suffers from $m = 0$, and $m = 1$ MHD instabilities, as can be shown via normal-mode analysis or an energy principle, as well as large parallel heat (end) losses, and the device was largely abandoned as a reactor concept because it was determined to be impossible to generate a fusing Z-pinch which lived long enough to break-even.

Still, the Z-Pinch remains the most promising magnetic confinement fusion (MCF) configuration because of its lack of need for external magnets, small form-factor, and unity beta[3] which makes it the simplest, and most cost-advantageous device, from an engineering perspective, when compared to toroidal configurations like the tokamak, or stellarator. In addition to their large form factor, and expensive external components, tokamaks also suffer from disruptions caused by runaway electrons. This last part is a serious problem for a "backbone reactor", meaning one which serves to provide base-band power for a modern energy grid, as it will either require the storage of sufficient electrical energy to maintain grid operation during disruptions, or multiple tokamaks would be required in a node, thereby further increasing the cost, and complexity of the plant.

Shear-Flow Stabilization

Modern Z-pinch fusion science also benefits from joinder with a stabilized form of the Z-pinch based on shear-flow-driven phase mixing of the different instabilities that allows a pinch lifetime which exhibits gross stability for many Alfven transit times[14]. Previous successful attempts to stabilize the Z-pinch involved the usage of wall image currents, hard-cores, or external arrays of magnetic coils to produce a stable confinement. None of these solutions are "power plant friendly" as, respectively, they will either lead to unsustainably short service lifetimes due to the enhanced melting of the wall, increased expense and operational downtime from the need for hard-core procurement and maintenance, and in general just increase the engineering costs, and complexity while presenting a set of new problems which lead the Z-pinch away from what makes it so promising, if stabilized in a manner independent of the aforementioned problematic mechanisms. Which, it has been[5].

The modern, shear-flow stabilized (SFS) Z-Pinch is currently being developed at Zap Energy, and the FuZE device is currently the subject of a number of computational studies which focus on simulating the plasma using multi-fluid models[15]. These studies are closely coupled to theoretical work on the subject, where the leading thought is to model the pinch using the marginally-stable equilibrium of Kadomtsev[16]. Experimental observations of FuZE show a rotating, turbulent pinch with a lifetime that is on the order of 1,000's of Alfven times, indicating the achievement of a quasi-equilibrium Z-pinch whose base flow possesses a non-uniform character. This magnetic stability arises from a shear flow in the axial plasma velocity of the axisymmetric equilibrium, meaning,

$$\frac{\mathrm{d}u_z}{\mathrm{d}r} > 0.1 k V_A \tag{26}$$

where $k = \frac{2\pi}{L}$ is naturally the axial wavenumber of the destabilizing mode, and $V_A = \frac{B}{\sqrt{\rho\mu}}$ is the velocity of

Alfven waves, i.e., transverse disturbances in the magnetic field which play a fundamental role in the plasma dynamics of MHD turbulence because they can travel in the direction of a field line while possessing an arbitrary waveform. The above expression can be manipulated into the form,

$$\frac{\mathrm{d}u_z}{\mathrm{d}r} > \sqrt{\frac{\mu}{\rho}}\frac{\pi B\sigma u}{5R_m} \tag{27}$$

Taking the ideal limit, $R_m \to \infty$, we arrive at the ideal condition,

$$\frac{\mathrm{d}u_z}{\mathrm{d}r} > 0 \tag{28}$$

A couple of notes must be made at this junction. Strictly-speaking, the above limit-taking process to reach an ideal situation is not the same thing as reaching that ideal situation via an infinite conductivity, $\lim_{\sigma\to\infty} R_m = \infty$. The latter of course being the situation by which fusion plasma scientists accord ideality to a fusion plasma on the basis of the high temperatures. Instead, the argument for ideal behavior here is based directly on the consideration of an infinitely long plasma column.

Bennett Pinch

Let us consider a Z-pinch where Equation (22) is described by,

$$J_z(r) = \frac{-en_0u_{z,0}}{(1+\xi^2r^2)^2} \tag{29}$$

which is the classic Bennett current, and can be inserted into Ampere's Law, Equation (19), then integrated via u-substitution or symbolic computation to yield the azimuthal magnetic field that provides the magnetic tension,

$$B_\theta(r) = -\frac{A}{2}\frac{r}{(1+\xi^2r^2)} \tag{30}$$

$$A = \mu_0 en_0 u_{z,0} \tag{31}$$

For a classic Bennett Pinch, this is enough to completely solve the entire system as the plasma number density has already been specified. Note that due to the uniform flow velocity this flow possesses identically zero vorticity,

$$\vec{\omega} = \nabla \times \vec{u} \tag{32}$$

and note as well that the magnetic tension is absent any singularities, but also gives a trivial answer for the field in the plasma core. Normalized profiles of these quantities are plotted in Figures (1), (2), and (3).

An analytic form for the plasma pressure of a Bennett Pinch can be integrated from the equation of motion with a suitable choice for the pressure of the core plasma, p_0,

$$p(r) = p_0 - \frac{A^2}{8\mu_0}r^2\frac{2+\xi^2r^2}{(1+\xi^2r^2)^2} \tag{33}$$

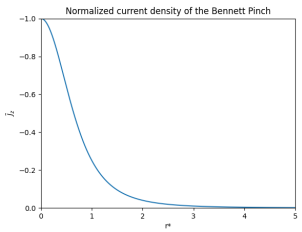

Figure 1. Normalized profile of the plasma current density for a Bennett Pinch, Equation (29). $\tilde{J}_z = \frac{J_z}{en_0u_{z,0}}$, and $r^* = \frac{r}{L^*} = r\xi$. The key feature to notice is the evanescence of the profile over a handful of scale-lengths without the need for any piecewise constructions that introduce discontinuities in the solution.

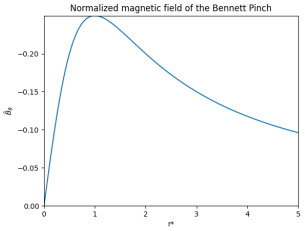

Figure 2. Normalized profile of the magnetic field for a Bennett Pinch, Equation (30), with $\tilde{B}_\theta = \frac{\xi}{A}B_\theta$. Note the need to introduce an extra factor of ξ into the form in order to properly normalize the length, completely. Outside of the region where the bulk plasma current goes to zero the magnetic field goes as $\sim \frac{1}{r}$ while inside this region the shape of the field is influenced by the nonlinear plasma current. Comparison with the other normalized profiles will convince that this $\frac{1}{r}$-dependence is a much slower falloff, comparatively. Also, observe that the theory gives a trivial solution for the value of the core magnetic field.

and the profile is plotted in Figure (4). Note that, unlike the Bennett Pinch, an adiabatic gas law cannot be invoked in the case of a Bennett Vortex as it would violate the requirement that a Bennett Vortex has for a uniform density, so an ideal gas law must then be spec-

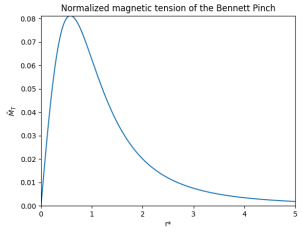

Figure 3. Normalized profile of the magnetic tension for a Bennett Pinch, $M_T = \frac{B_\theta^2}{\mu r}$. The normalized profile displayed here is given by $\tilde{M}_T = M_T\frac{\mu\xi}{A^2} = \frac{\tilde{B}_\theta^2}{r^*}$. The lack of singularity in the profile is due to the nonlinear dependence of B_θ, i.e., the Bennett profile.

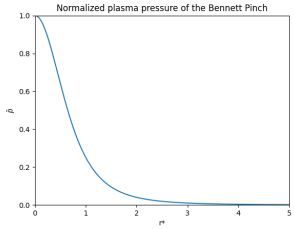

Figure 4. Normalized plasma pressure of the Bennett Pinch as a function of the dimensionless coordinate $r^* = r\xi$. $\tilde{p} = \frac{p}{p_0}$ is plotted here, and there is a specific requirement for $p_0 = \frac{A^2}{8\xi^2\mu}$ to achieve the dimensionless form. This amounts to the trivial constraint that $T \neq 0$ which is an uninteresting limit in the theory because it represents a plasma with zero thermal energy, i.e., a trivial one as far as fusion plasma physics is concerned.

ified to close the system of equations. This translates into a temperature gradient, rather than a density, and consequently the Bennett parameter, $b \to b(r)$, now becomes spatially-dependent since it is directly related to an inverse temperature. This feature is the main difference between a Bennett Vortex and the classic Bennett Pinch equilibrium.

Bennett Vortices

Bennett Vortices are a phenomenon which can be observed in the axial velocity profiles of the ZaP, and ZaP-HD experiments, and for whom the cubic vortex theory gives reasonable agreement across the span of observable quantities related to magnetic structure and stability. This agreement extends to order of magnitude calculations for total current, magnetic field, and plasma pressure, in addition to having a magnetic null on the axis, and an extremum at the pinch radius. Notably, the pure-flow cubic vortex diverges in regard to temperature profile, and density profile, but the axial velocity profile is seen to appear locally. Most notably it predicts the shear very accurately[17] for the case when the temperature is cubic,

$$T = C_T r^3 = \frac{T_p}{r_p^3} r^3 \tag{34}$$

because there is an analytic equilibrium for the "pure flow" case whose normalized profiles are plotted in Figures (), and which are described in closed-form by,

$$n = n_0 \tag{35}$$

$$\vec{J} = J_z(r)\hat{z} = \frac{-en_0u_{z,0}}{(1+\xi^2r^2)^2} = \frac{-en_0u_{z,0}T^2}{(T+C_Bn_0r^2)^2}\hat{z} \tag{36}$$

$$= \frac{-en_0u_{z,0}C_T^2r^6}{(C_Tr^2)^2(r+C_{B,T})^2}\hat{z} \tag{37}$$

$$= -en_0u_{z,0}\frac{r^2}{(r+C_{B,T})^2}\hat{z} \tag{38}$$

$$\vec{B}_\theta(r) = B_\theta(r)\hat{\theta} = \frac{-\mu_0en_0u_{z,0}}{2r(r+C_{B,T})}f(r,C_{B,T})\hat{\theta} \tag{39}$$

$$f = r^3 - 3r^2C_{B,T} \tag{40}$$

$$- 6rC_{B,T}^2(1+\ln\left(\frac{C_{B,T}}{r+C_{B,T}}\right)) \tag{41}$$

$$- 6C_{B,T}^3(\ln\left(\frac{C_{B,T}}{r+C_{B,T}}\right) \tag{42}$$

$$f = f_1 + f_2 + f_3 + f_4 \tag{43}$$

$$p(r) = p_0 - \frac{\mu_0(en_0u_{z,0})^2}{4(r+C_{B,T})^2}\Big[r^4 - 10r^3C_{B,T} + \dots$$
$$+ 3r^2C_{B,T}^2\Big(- 13 + 2\ln^2(C_{B,T}) + 6\ln(r+C_{B,T})$$
$$+ 2\ln^2(r+C_{B,T}) - 2\ln(C_{B,T})(3+2\ln(r+C_{B,T}))\Big)$$
$$+ 6rC_{B,T}^3\Big(- 5 + 2\ln^2(C_{B,T}) + 8\ln(r+C_{B,T})$$
$$+ 2\ln^2(r+C_{B,T}) - 4\ln(C_{B,T})(2+\ln(r+C_{B,T})\Big)$$
$$+ 6C_{B,T}^4\Big(\ln^2(C_{B,T}) + \ln(r+C_{B,T})(5$$
$$+ \ln(r+C_{B,T})) - \ln(C_{B,T})(5+2\ln(r+C_{B,T}))\Big)\Big]$$

$$I_{encl}(r_p) = \int_{A_p}\vec{J}\cdot d\vec{A}$$
$$= \int_0^{2\pi}\int_0^{r_p} rJ_z(r)drd\theta$$
$$= 2\pi en_0u_{z,0}\int_0^{r_p}\frac{r^3}{(r+C_{B,T})^2}dr$$
$$= \frac{2\pi en_0u_{z,0}}{2(r_p+C_{B,T})}\Big(r_p^3 - 3r_p^2C_{B,T}$$
$$- 6r_pC_{B,T}^2(1+\ln\left(\frac{C_{B,T}}{r_p+C_{B,T}}\right))$$
$$- 6C_{B,T}^3\ln\left(\frac{C_{B,T}}{r_p+C_{B,T}}\right)\Big)$$

with the vortex constant,

$$C_{B,T} = \frac{C_Bn_0}{C_T} \tag{44}$$

$$= \frac{C_Bn_0}{T_p}r_p^3 \tag{45}$$

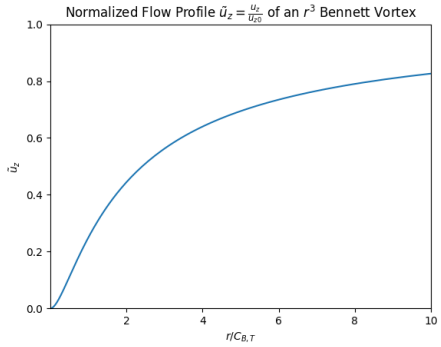

Figure 5. Normalized axial velocity profile of a cubic Bennett Vortex. Note the parabolic character close to the origin of the pinch axis, and the saturation at the edge flow value far from it.

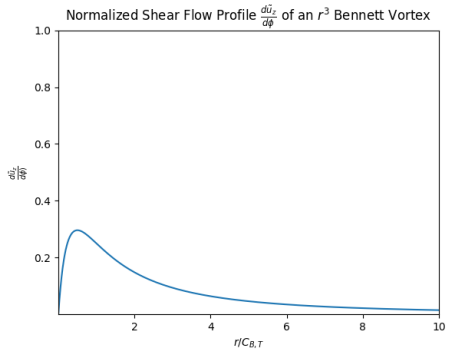

Figure 6. Normalized shear of a cubic, pure-flow, Bennett Vortex. Note how quickly the peak shear is reached, explaining how the SFS equilibrium can form for small length-scales. Calculations accurately reproduce the shear values observed in contemporary devices.

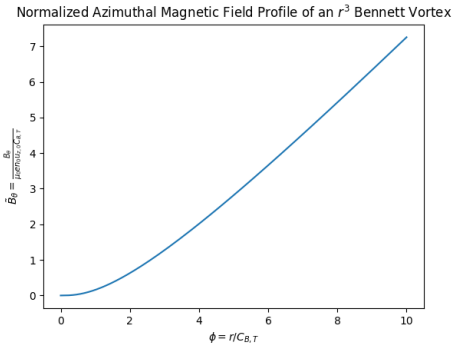

Figure 7. Linear view of the normalized magnetic field of a cubic Bennett Vortex. Note how the profile possesses an on-axis magnetic null, and an extrema at the pinch radius, both features of which are observed in real SFS devices.

where the Bennett constant, C_B, is

$$C_B = \frac{\mu_0 e^2 u_{z,0}^2}{16 k_B} \tag{46}$$

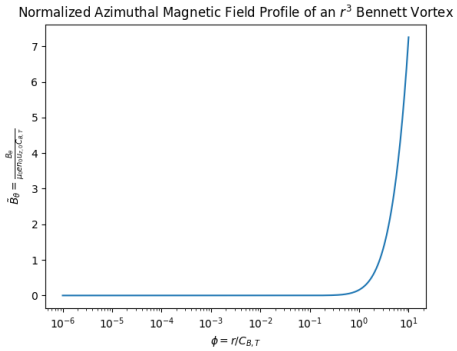

Figure 8. Log view of the normalized magnetic field of a cubic Bennett Vortex. Order of magnitude estimates are obtained when calculations are performed with FuZE operating conditions

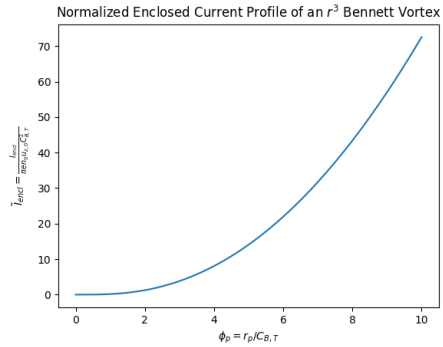

Figure 9. Normalized enclosed current of a cubic Bennett Vortex. Order of magnitude estimates are returned when calculations are performed with values characteristic of experimental operating conditions

For a cubic Bennett Vortex the edge flow speed is related to $u_{z,0}$,

$$u_{edge} = u_z(r_p) = u_{z,0} \frac{r_p^2}{(r_p + C_{B,T})^2} \tag{47}$$

when $C_{B,T}$ is small they are approximately the same value. $C_{B,T}$ scales with the pinch radius cubed so in modern Z-Pinch devices it is frequently a good approximation to make as can be seen in Figures (10), (11), (12), (13), and (14), The smallness of $C_{B,T}$ is of great importance to the physics of a cubic Bennett Vortex because it allows for the simplification of the complicated pressure, and magnetic field expression.

Of course, the cubic, pure-flow, vortex does not completely describe the observations seen in modern SFS fusion devices. For example, the density is not uniform, and these results are obtained by treating the edge plasma temperature of the cubic temperature profile as being the core electron plasma temperature. While this is strange, the theory also predicts that these SFS cubic vortices do not need all that much space to develop in the operating

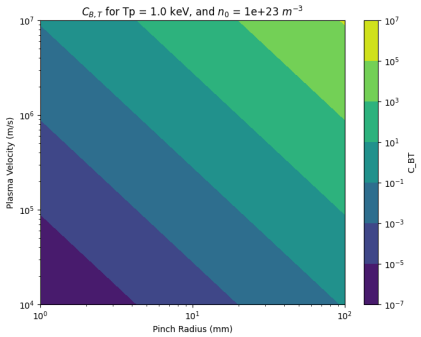

Figure 10. Log-log contour plot of $C_{B,T}$ for a FuZE-like cubic vortex with an edge plasma temperature of $T = 1$ [keV].

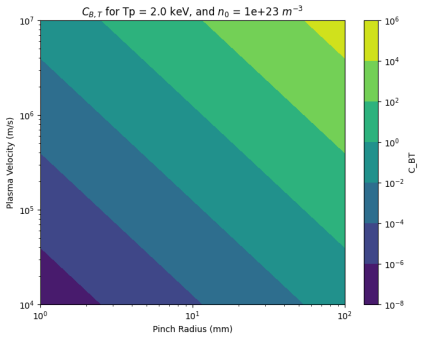

Figure 11. Log-log contour plot of $C_{B,T}$ for a FuZE-like cubic vortex with an edge plasma temperature of $T = 2$ [keV].

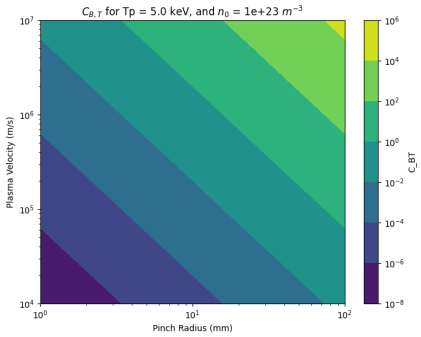

Figure 12. Log-log contour plot of $C_{B,T}$ for a FuZE-like cubic vortex with an edge plasma temperature of $T = 5$ [keV].

conditions of contemporary experiments, as can be seen from Figures (15), (16), (17), (18), and (19), so it is not an incoherent leap of faith to treat the system in this way.

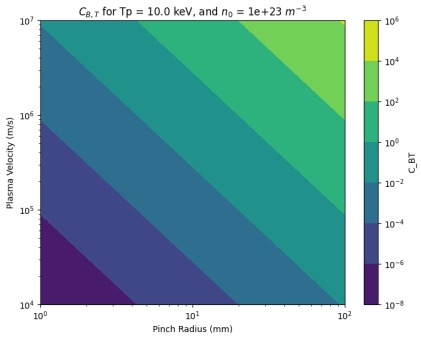

Figure 13. Log-log contour plot of $C_{B,T}$ for a FuZE-like cubic vortex with an edge plasma temperature of $T = 10$ [keV].

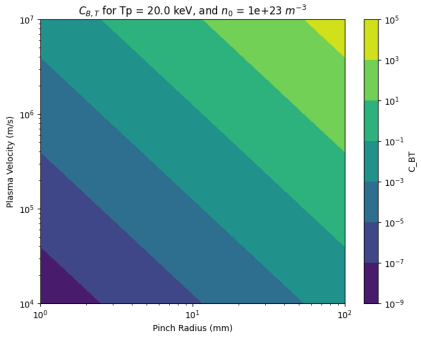

Figure 14. Log-log contour plot of $C_{B,T}$ for a FuZE-like cubic vortex with an edge plasma temperature of $T = 20$ [keV].

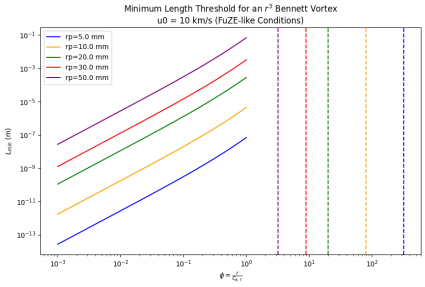

Figure 15. Minimum length required for an r^3 Bennett Vortex to be SFS for FuZE-like conditions with an edge flow speed of $u_{z,0} = 10$ $[km\ s^{-1}]$. Each colored vertical line is the corresponding location of ϕ_p, which is the dimensionless boundary to the Bennett Vortex.

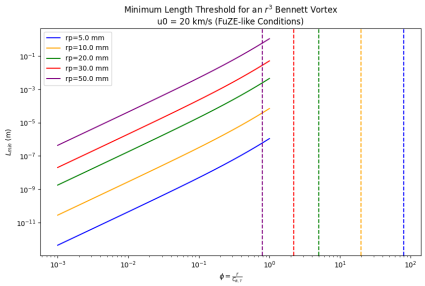

Figure 16. Minimum length required for an r^3 Bennett Vortex to be SFS for FuZE-like conditions with an edge flow speed of $u_{z,0} = 20$ $[km\ s^{-1}]$. Each colored vertical line is the corresponding location of ϕ_p, which is the dimensionless boundary to the Bennett Vortex.

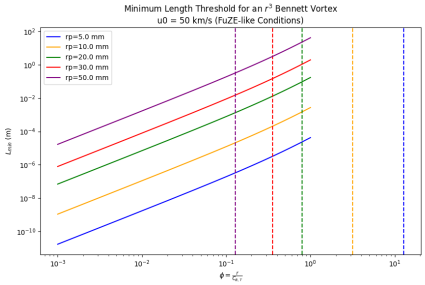

Figure 17. Minimum length required for an r^3 Bennett Vortex to be SFS for FuZE-like conditions with an edge flow speed of $u_{z,0} = 50$ $[km\ s^{-1}]$. Each colored vertical line is the corresponding location of ϕ_p, which is the dimensionless boundary to the Bennett Vortex.

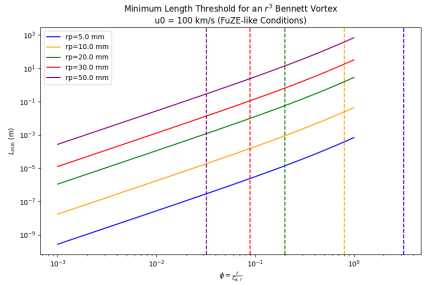

Figure 18. Minimum length required for an r^3 Bennett Vortex to be SFS for FuZE-like conditions with an edge flow speed of $u_{z,0} = 100$ $[km\ s^{-1}]$. Each colored vertical line is the corresponding location of ϕ_p, which is the dimensionless boundary to the Bennett Vortex.

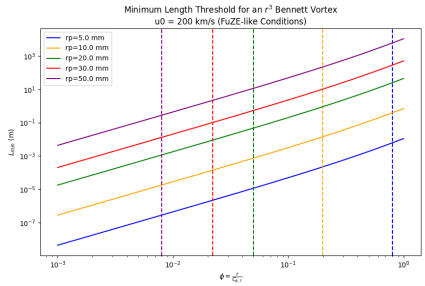

Figure 19. Minimum length required for an r^3 Bennett Vortex to be SFS for FuZE-like conditions with an edge flow speed of $u_{z,0} = 200$ $[km\ s^{-1}]$. Each colored vertical line is the corresponding location of ϕ_p, which is the dimensionless boundary to the Bennett Vortex.

RESULTS

Mixed Bennett Vortices

The magnetohydrodynamic theory of a mixed Bennett Vortex, where

$$n(r) = \frac{n_0 T^\nu}{(T + C_B n_0 r^2)^\nu} P(n, \alpha, \beta) \tag{48}$$

$$u_z(r) = \frac{u_{z,0} T^\chi}{(T + C_B n_0 r^2)^\chi} G(n, \alpha, \beta) \tag{49}$$

has an analytic solution for the cubic temperature case, $T = \frac{T_p}{r_p^3} r^3$, because the current density,

$$\vec{J} = \frac{-e n_0 u_{z,0} T^{\nu+\chi}}{(T + C_B n_0 r^2)^{\nu+\chi}} P(n, \alpha, \beta) G(n, \alpha, \beta) \hat{z} \tag{50}$$

$$= -\frac{-e n_0 u_{z,0} T^2}{(T + C_B n_0 r^2)^2} \hat{z} \tag{51}$$

keeps the same form, and therefore the magnetic field, and plasma pressure, remain the same as they do when the flow velocity carries the nonlinearity entirely, i.e., a "pure-flow" cubic vortex, provided there is a unity product coupling, such as,

$$P(n, \alpha, \beta) = (\alpha\beta)^n \tag{52}$$

$$G(n, \alpha, \beta) = (\alpha\beta)^{-n} \tag{53}$$

which gives, among others,

$$UC[P, G; n, \alpha, \beta] = P(n, \alpha, \beta) G(n, \alpha, \beta) = 1 \tag{54}$$

and

$$\nu + \chi = 2 \tag{55}$$

These forms give the analysis greater range for providing insight into, and exploring, how the weighting of edge density versus edge flow speed in a Bennett Vortex influences the performance of the plasma. Additionally, they allow the investigation of a particular flavor

of analytic vortex to be tailored based on observed data which in reality is non-uniform both in flow profile and density[14][18].

Uniform Mixed Unity Cubic Vortex

Let us start by considering the uniform case where,

$$\nu = \chi = 1 \tag{56}$$

and,

$$P(n, \alpha, \beta) = G(n, \alpha, \beta) = 1 \tag{57}$$

which leads to density and flow profiles of the form,

$$n(r) = \frac{n_0 T(r)}{T(r) + C_B n_0 r^2} \tag{58}$$

$$u_z(r) = \frac{u_{z,0} T(r)}{T(r) + C_B n_0 r^2} \tag{59}$$

The r^3 Mixed Bennett Vortex is guaranteed to have a solution for this case because the form of the plasma current is unchanged from the r^3 pure-flow Bennett Vortex, and therefore the magnetic field will be the same, as will the plasma pressure.

The most important consideration is the shear,

$$\frac{\mathrm{d}u_z}{\mathrm{d}r} = u_{z,0}\left(-\frac{r}{(r + C_{B,T})^2} + \frac{1}{r + C_{B,T}}\right) \tag{60}$$

$$= u_{z,0} \frac{C_{B,T}}{(r + C_{B,T})^2} \tag{61}$$

$$\therefore \frac{\mathrm{d}\tilde{u}_z}{\mathrm{d}r} = \frac{C_{B,T}}{u_{z,0}} \frac{\mathrm{d}u_z}{\mathrm{d}r} = \frac{1}{(\phi + 1)^2}$$

which is shown in Figure (20) The maximal shear evidently occurs at the pinch axis, and the minimal as the dimensionless radius goes to ∞. The SFS criterion[4],

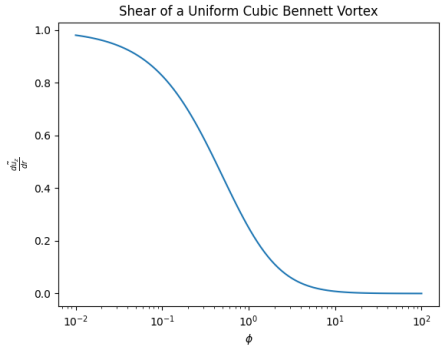

Figure 20. The shear of a uniform cubic Bennett vortex.

$$\frac{\mathrm{d}u_z}{\mathrm{d}r} > 0.1 k V_A \tag{62}$$

is then,

$$\frac{u_{z,0} C_{B,T}}{(r + C_{B,T})^2} > \frac{\pi}{5L} \frac{B_\theta(r)}{\sqrt{\rho(r)\mu_0}} \tag{63}$$

recalling that the magnetic field of *any* cubic vortex whose profiles restore the form of the pure-flow cubic vortex's current density, is,

$$\vec{B} = B_\theta(r)\hat{\theta} = -\frac{\mu_0 e n_0 u_{z,0,}}{2r(r + C_{B,T})}\Bigg(r^3 - 3C_{B,T} r^2 \tag{64}$$

$$- 6r C_{B,T}^2 \left(1 + \ln\left(\frac{C_{B,T}}{r + C_{B,T}}\right)\right. \tag{65}$$

$$\left. - 6C_{B,T}^3 \ln\left(\frac{C_{B,T}}{r + C_{B,T}}\right)\right)\hat{\theta} \tag{66}$$

$$= -\frac{\mu_0 e n_0 u_{z,0,}}{2r(r + C_{B,T})} f(r, C_{B,T})\hat{\theta} \tag{67}$$

Re-arranging Equation (63) to isolate the pinch length on the left, we obtain,

$$L > \frac{e\pi}{10} \frac{1}{C_{B,T}} \left(\frac{r + C_{B,T}}{r}\right)^{\frac{3}{2}} \sqrt{\frac{n_0 \mu_0}{m_H}} f(r, C_{B,T}) \tag{68}$$

We can rewrite this in terms of the dimensionless plasma radius, ϕ, and collect any left-over terms on the left into a dimensionless pinch length, to arrive at a lower bound for what this dimensionless pinch length needs to be for the cubic vortex to SFS,

$$\tilde{L} > \left(\frac{\phi + 1}{\phi}\right)^{\frac{3}{2}} \Big[\phi^3 - 3\phi^2 - 6\phi \tag{69}$$

$$+ 6\phi \ln(\phi + 1) + 6 \ln(\phi + 1)\Big] \tag{70}$$

$$\tilde{L} = L \frac{10\sqrt{m_H}}{e\pi\sqrt{\mu_0 n_0} C_{B,T}^2} \tag{71}$$

which is plotted in Figure (**??**) alongside the equivalent expression for the pure-flow cubic vortex, To determine the behavior of $\tilde{L}$ at the origin, L'Hopitals rule must be applied twice in order to completely eliminate the singularity in the denominator. These derivatives are computed with Wolfram Mathematica, and listed in Appendix A. The result obtained is,

$$\tilde{L}(0) = \lim_{\phi \to 0} \tilde{L} = \lim_{\phi \to 0} \frac{1}{3} \sqrt{\frac{\phi}{1 + \phi}} \Big(- 336 - 666\phi - 21\phi^2$$

$$+ 63\phi^3 - 90(4 + 5\phi) \ln(1 + \phi)\Big)$$

$$= 0$$

notice in the above that $\tilde{L}$ will be negative for a certain extent around ϕ, which implies that the length of the pinch necessary for an SFS vortex to develop close to the pinch axis can be any arbitrary positive value, i.e., that this kind of cubic vortex can also form SFS states for arbitrarily small pinch lengths arbitrarily close the pinch axis. This can be seen in Figure (22)

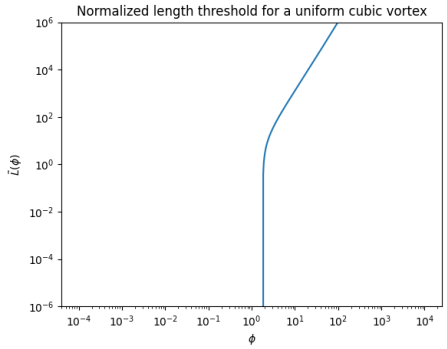

Figure 21. Loglog plot of the dimensionless threshold length which is required for a uniform cubic vortex to form an SFS state. Note how quickly the length increases with plasma radius, but also the abrupt transition and drop to small values as ϕ approaches unity.

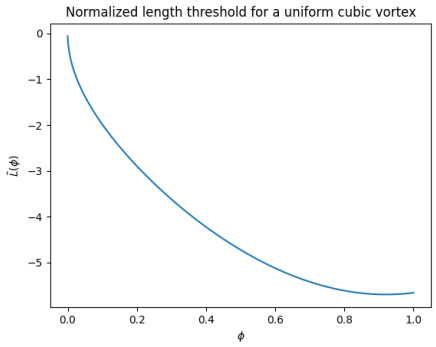

Figure 22. Linear view of $\tilde{L}$ for a uniform vortex close to origin alongside the pure-flow case

General Mixed Unity Cubic Vortex

In general, we must analyze density and axial flow profiles of the forms given by Equation (48), and (49, with the constraints described previously on ν, χ, and the unity coupling. Neglecting the unity coupling for the moment, i.e., setting,

$$P(n,\alpha,\beta) = G(n,\alpha,\beta) = 1 \tag{72}$$

then we have,

$$n(r) = \frac{n_0 T^{\nu}(r)}{(T(r) + C_B n_0 r^2)^{\nu}}$$
$$u_z(r) = \frac{u_{z,0} T^{\chi}(r)}{(T(r) + C_B n_0 r^2)^{\chi}}$$

which has an analytic solution for the cubic temperature case because the constraints will result in a form to the Bennett Current which is the same as that of a cubic vortex, therefore the magnetic field and plasma pressure will be the same as well even though the form of the profiles can be very different.

The shear reads,

$$\frac{\mathrm{d}u_z}{\mathrm{d}r} = u_{z,0}\frac{\mathrm{d}}{\mathrm{d}r}\left(\frac{1}{C_T^{\chi} r^{2\chi}}\frac{C_T^{\chi} r^{3\chi}}{(r+C_{B,T})^{\chi}}\right) \tag{73}$$
$$= u_{z,0}\frac{\mathrm{d}}{\mathrm{d}r}\left(\frac{r^{\chi}}{(r+C_{B,T})^{\chi}}\right) \tag{74}$$
$$= u_{z,0}\left(\chi\frac{r^{\chi-1}}{(r+C_{B,T})^{\chi}} - \chi\frac{r^{\chi}}{(r+C_{B,T})^{\chi+1}}\right) \tag{75}$$

There are two avenues to consider for further attack. The first is what the constraint on χ is which leads to zero shear, other than $\chi = 0$ of course which reduces to the "pure-density" form of the classic Bennett Pinch. The second being what choice of χ maximizes the shear as the sustainment of a shear above the plasma threshold is required for the stability of the Z-Pinch device, and is the primary concern to elongating the fusion burn time.

The first question is addressed via,

$$u_{z,0}\chi\left(\frac{r^{\chi-1}}{(r+C_{B,T})^{\chi}} - \frac{r^{\chi}}{(r+C_{B,T})^{\chi+1}}\right) = 0 \tag{76}$$
$$\therefore \frac{r^{\chi-1}}{(r+C_{B,T})^{\chi}} = \frac{r^{\chi}}{(r+C_{B,T})^{\chi+1}} \tag{77}$$

$$\rightarrow r = r + C_{B,T} \tag{78}$$
$$\rightarrow C_{B,T} = 0 = \frac{\mu_0 e^2 u_{z,0}^2 n_0 r_p^3}{16 k_B T_p} \tag{79}$$

This is a remarkably strange condition on there being no shear, however, for a real SFS plasma it will never be satisfied so in practice there will always be some shear except in the case when the flow is uniform. Nevertheless, it is instructive to examine the various limits in which $C_{B,T}$ goes to 0.

The first is when the temperature runs to ∞,

$$\lim_{T_p\to\infty} C_{B,T} \to 0 \tag{80}$$

which is just a reflection of there being an "ultraviolet catastrophe" in our classical theory. It can also be thought of as a reflection of the Kruskal-Shafranov limit on the amount of current which a plasma can handle stably. As the current increases through the pinch, so too does the edge plasma temperature due to resistive heating, and in the limit of infinitely large current we have a temperature that runs our $C_{B,T}$ to zero, causing a collapse of the shear.

The other interesting limit is when the pinch radius goes to zero, as this constant scales most strongly with pinch radius,

$$\lim_{r_p\to 0} C_{B,T} \to 0 \tag{81}$$

Of course, this limit is not troublesome to our cubic vortex theory as a pinch with a zero pinch radius is no problem at all. It does however suggest a mechanism behind

a failure mode of a cubic Bennett vortex. Namely, that if the pinch radius grows too small then the shear will collapse.

Addressing the second question posed, that of where the shear is maximized in space, begins by considering the shear of the shear,

$$\frac{\mathrm{d}^2 u_z}{\mathrm{d}r^2} = u_{z,0}\chi\frac{\mathrm{d}}{\mathrm{d}r}\Big(r^{\chi-1}(r+C_{B,T})^{-\chi} - r^{\chi}(r+C_{B,T})^{-\chi-1}\Big) = 0$$

$$\begin{aligned}\therefore\ &(\chi-1)r^{\chi-2}(r+C_{B,T})^{-\chi} \\ &- 2\chi r^{\chi-1}(r+C_{B,T})^{-\chi-1} \\ &+ (\chi+1)r^{\chi}(r+C_{B,T})^{-\chi-2} = 0 \\ \rightarrow\ &(\chi-1)(r+C_{B,T})^2 - 2\chi r(r+C_{B,T}) + (\chi+1)r^2 = 0\end{aligned}$$

Which can be further expanded, and simplified to yield a relationship for the dimensionless coordinate,

$$\phi = \frac{r}{C_{B,T}} \tag{82}$$

at which the shear is maximized,

$$\phi_{max}(\chi) = \frac{\chi-1}{2} \tag{83}$$

For the pure-flow, $\chi = 2$, case the max shear occurs at,

$$\frac{\mathrm{d}^2\tilde{u}_z}{\mathrm{d}\phi^2} = \frac{\mathrm{d}}{\mathrm{d}\phi}\Big(2\phi(\phi-1)^{-2} - 2\phi^2(\phi+1)^{-3}\Big) \tag{84}$$

$$= 2(\phi+1)^{-2} - 8\phi(\phi+1)^{-3} + 6\phi^2(\phi+1)^{-4} \tag{85}$$

$$= 2(\phi+1)^2 - 8\phi(\phi+1) + 6\phi^2 \tag{86}$$

$$= 0 \tag{87}$$

an expression which can be expanded and terms collected to yield,

$$\phi_{max}(\chi=2) = \frac{1}{2} \tag{88}$$

which agrees with Equation (83).

We also wish to know where the shear is maximized in terms of χ as we have significant freedom to let χ range provided that $\chi + \nu = 2$ is maintained. This derivative is substantially more complicated, but made easy with Mathematica,

$$\frac{\mathrm{d}}{\mathrm{d}\chi}\frac{\mathrm{d}u_z}{\mathrm{d}r} = u_{z,0}C_{B,T}\frac{r^{\chi-1}}{(r+C_{B,T})^{\chi+1}}\Big(1 + \chi\ln\Big(\frac{r}{r+C_{B,T}}\Big)\Big) = 0$$

$$\rightarrow \chi(\ln(\phi) - \ln(\phi+1)) = -1 \tag{89}$$

$$\therefore \chi = \frac{1}{\ln(\phi+1) - \ln(\phi)} \tag{90}$$

the above is a result which is very odd as it indicates that the χ which results in an extremum shear is dependent on the position in the plasma. Furthermore, one of the main challenges with cubic vortex theory is the awkwardness of the dimensionless coordinate, ϕ, as it would be much preferable to write things in terms of a dimensionless coordinate that is easily interpretable, such as the ratio of coordinate radius to pinch radius. However, this is generally not possible because of the structure of the theory so any interpretation must be made in the context of a distinct set of plasma conditions so that the pinch radius can be marked on the plot as the vortex is only valid inside the pinch. Lastly, Equation (90) is known to give the maximal shear form-power because the other solution is $\chi = 0$, which clearly results in a state of zero shear, i.e., uniform flow.

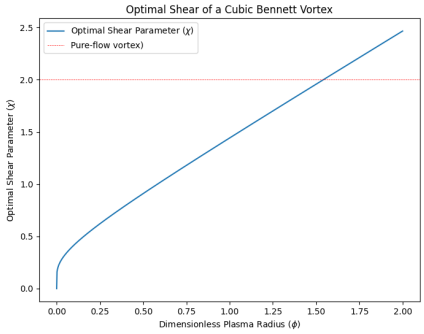

Figure 23. Plot of Equation (90), showing the trend in optimal flow-power χ as a function of dimensionless radial coordinate. While such a graph is difficult to interpret alone, due to the structure of the dimensionless coordinate involving a cubic power of pinch radius, in the case of a specific set of plasma conditions it will provide a clear picture of what flow-power gives the maximally shearing vortex form at a point in the plasma.

FUTURE WORK AND CONCLUSION

The cubic Bennett Vortex has an analytic equilibrium, therefore no matter how the Bennett nonlinearity is distributed amongst the flow-power, χ, and the density-power, ν, a cubic vortex will still have an analytic equilibrium so long as the current density is equal to the Bennett Current of a cubic vortex. Consequentially, various product forms can be coupled to the density and flow, e.g.,

$$P(n,\alpha,\beta) = (\alpha\beta)^n \tag{91}$$

$$G(n,\alpha,\beta) = (\alpha\beta)^{-n} \tag{92}$$

and so long as $PG = 1$, these forms will preserve the analytic cubic vortex current while allowing for the study of the impact which these weightings have on the plasma performance. The impact of these different forms on the

overall plasma performance has not been studied in this work as the focus was on the power-forms.

By studying the flow-power form, χ, conditions for where maximal and minimal shear occur in a cubic vortex were derived. The first is when

$$C_{B,T} = \frac{\mu_0 n_0 e^2 u_{z,0}^2 r_p^3}{16 k_B T_p} = 0 \tag{93}$$

which can be achieved in two main ways. The first when the temperature runs to ∞, a reflection of an ultraviolet catastrophe in the classical theory, as well as a reminder of the Kruskal-Shafranov limit on the amount of current which a stable plasma can handle. The second is when the pinch radius goes to 0, which is of course not a problem from a theoretical perspective as a pinch problem with no pinch is no problem at all unless there is an SFS Bennett Vortex forming arbitrarily close to its axis.

It should be said that the pure-flow cubic theory of a Bennett Vortex is most accurate at predicting the shear which will be observed in an SFS fusion device, while its predictions of current, magnetic field, and plasma pressure are generally good order of magnitude estimates which can give insight into the design of a reactor and rocket based on the theory.

APPENDIX A: UNIFORM $\tilde{L}(0)$ DERIVATIVES

To determine the value of $\tilde{L}$ at the origin, L'Hopitals rule must be applied twice because the first application,

$$\lim_{\phi\to 0} \tilde{L}(\phi) = \lim_{\phi\to 0} \frac{\mathrm{d}\tilde{L}_{num}}{\mathrm{d}\phi} \Big/ \frac{\mathrm{d}\tilde{L}_{den}}{\mathrm{d}\phi} \tag{94}$$

where,

$$\begin{aligned}
\frac{\mathrm{d}\tilde{L}_{num}}{\mathrm{d}\phi} &= (1+\phi)^{3/2}\bigg(3\phi^2 - 6\phi - \frac{30\phi}{\phi+1} \\
&\quad - 6(1+5\ln(1+\phi))\bigg) \\
&\quad + \frac{3}{2}\sqrt{1+\phi}\bigg(\phi^3 - 3\phi^2 - 6\phi(1+5\ln(1+\phi))\bigg) \\
\frac{\mathrm{d}\tilde{L}_{den}}{\mathrm{d}\phi} &= \frac{3}{2}\sqrt{\phi}
\end{aligned}$$

which obviously still has a singularity in it. So, we must take a second pair of derivatives,

$$\begin{aligned}
\frac{\mathrm{d}^2\tilde{L}_{num}}{\mathrm{d}\phi^2} &= \frac{1}{4\sqrt{1+\phi}}\bigg(-336 - 666\phi - 21\phi^2 \\
&\quad + 63\phi^3 - 90(4+5\phi)\ln(1+\phi)\bigg) \\
\frac{\mathrm{d}^2\tilde{L}_{den}}{\mathrm{d}\phi^2} &= \frac{3}{4}\phi^{-1/2}
\end{aligned}$$

[1] J. Allen and L. Simons, The bennett pinch for non-relativistic electrons, J. Plasma Phys., vol. 84 (2018).

[2] W. H. Bennett, Magnetically self-focussing streams, Physical Review, Volume 45 (1934).

[3] U. Shumlak, Z-pinch fusion, Journal of Applied Physics **127**, 200901 (2020), https://pubs.aip.org/aip/jap/article-pdf/doi/10.1063/5.0004228/20006426/200901_1_5.0004228.pdf.

[4] U. Shumlak and C. W. Hartman, Sheared flow stabilization of the $m = 1$ kink mode in Z pinches, Phys. Rev. Lett. **75**, 3285 (1995).

[5] U. Shumlak, R. P. Golingo, B. A. Nelson, and D. J. Den Hartog, Evidence of stabilization in the Z-pinch, Phys. Rev. Lett. **87**, 205005 (2001).

[6] U. Shumlak, B. A. Nelson, R. P. Golingo, S. L. Jackson, E. A. Crawford, and D. J. Den Hartog, Sheared flow stabilization experiments in the zap flow z pinch, Physics of Plasmas **10**, 1683 (2003), https://pubs.aip.org/aip/pop/article-pdf/10/5/1683/19271537/1683_1_online.pdf.

[7] R. P. Golingo, U. Shumlak, and B. A. Nelson, Formation of a sheared flow Z pinch, Physics of Plasmas **12**, 062505 (2005).

[8] D. J. Ampleford, S. N. Bland, M. E. Cuneo, S. V. Lebedev, D. B. Sinars, C. A. Jennings, E. M. Waisman, R. A. Vesey, G. N. Hall, F. Suzuki-Vidal, J. P. Chittenden, and S. C. Bott, Demonstration of radiation pulse-shaping capabilities using nested conical wire-array z-pinches, IEEE Transactions on Plasma Science **40**, 3334 (2012).

[9] U. Shumlak, B. Nelson, and B. Levitt, The sheared-flow-stabilized z-pinch approach to fusion energy, in *2023 IEEE International Conference on Plasma Science (ICOPS)* (2023) pp. 1–1.

[10] P. Davidson, *Introduction to Magnetohydrodynamics* (Cambridge University Press, 2017).

[11] P. Davidson, *Turbulence* (Cambridge University Press, 2015).

[12] J. P. Friedberg, *Ideal MHD* (Cambridge University Press, 2014).

[13] J. Huba, *NRL Plasma Formulary* (Naval Research Laboratory, 2013).

[14] U. Shumlak, C. S. Adams, J. M. Blakely, B. J. Chan, R. P. Golingo, S. D. Knecht, B. A. Nelson, R. J. Oberto, M. R. Sybouts, and G. V. Vogman, Equilibrium, flow shear and stability measurements in the Z-pinch, Nuclear Fusion **49**, 075039 (2009).

[15] E. T. Meier and U. Shumlak, Development of five-moment two-fluid modeling for z-pinch physics, Physics of Plasmas **28**, 092512 (2021), https://pubs.aip.org/aip/pop/article-pdf/doi/10.1063/5.0058420/13420598/092512_1_online.pdf.
[16] D. W. Crews, I. A. M. Datta, E. T. Meier, and U. Shumlak, The kadomtsev pinch revisited for sheared-flow-stabilized z-pinch modeling, IEEE Transactions on Plasma Science **52**, 4804 (2024).
[17] M. Russell, Bennett vorticity: a family of nonlinear shear-flow stabilized z-pinch equilibria, (2025).
[18] U. Shumlak, B. A. Nelson, E. L. Claveau, E. G. Forbes, R. P. Golingo, M. C. Hughes, R. J. Oberto, M. P. Ross, and T. R. Weber, Increasing plasma parameters using sheared flow stabilization of a z-pinch, Physics of Plasmas **24**, 055702 (2017), https://pubs.aip.org/aip/pop/article-pdf/doi/10.1063/1.4977468/15993954/055702_1_online.pdf.